

Thirring Solitons in the Presence of Dispersion

Alan R. Champneys

Department of Engineering Mathematics, University of Bristol, Bristol BS8 1TR, United Kingdom

Boris A. Malomed

Department of Interdisciplinary Studies, Faculty of Engineering, Tel Aviv University, Tel Aviv 69978, Israel

Mark J. Friedman

Department of Mathematics, University of Alabama, Huntsville, Alabama

(Received 9 September 1997; revised manuscript received 29 January 1998)

The effect of dispersion or diffraction on zero-velocity solitons is studied for the generalized massive Thirring model describing a nonlinear optical fiber with grating or parallel-coupled planar waveguides with misaligned axes. The Thirring solitons existing at zero dispersion/diffraction are shown numerically to be separated by a *finite gap* from three isolated soliton branches. Inside the gap, there is an infinity of multisoliton branches. Thus, the Thirring solitons are *structurally unstable*. In another parameter region (far from the Thirring limit), solitons exist everywhere. [S0031-9007(98)05954-7]

PACS numbers: 42.65.Tg, 03.40.Kf

The massive Thirring model (MTM) [1] is a completely integrable [2] Lorentz-invariant model of classical field theory, which supports exact soliton and multisoliton solutions [1]. A generalization of the MTM, which we call the optical model (OM), was introduced in [3,4] to describe interaction between right- and left-traveling waves in a nonlinear optical fiber with a grating. Resonant Bragg scattering and cross-phase modulation (CPM) give rise, respectively, to linear and nonlinear couplings between the two waves. OM additionally includes self-phase-modulation (SPM) nonlinear terms, making it *nonintegrable* and destroying Lorentz invariance. Nevertheless, a family of *exact* one-solitons can be found [3,4] with arbitrary velocity and internal amplitude (“soliton” hereafter means solitary wave, and “ n -soliton” is one with n peaks). Recently, Bragg solitons have been observed experimentally in a fiber with grating [5].

Both MTM and OM neglect dispersion of the medium, solitons being supported by an *effective dispersion* induced by the linear coupling. In physical media, however, material dispersion is present. The aim of this work is to examine the influence of such dispersion D on the Thirring solitons (TS). This first study treats only zero-velocity solitons, which are essentially the same in MTM and OM. Results for finite-velocity (*walking* [6]) solitons, to be presented elsewhere, are more complicated technically but not drastically different (see below). The zero-velocity solitons are most intriguing physically, as they imply complete dynamical self-trapping of light on the grating. We will conclude that TS are *structurally unstable*, being separated by a finite gap from the nearest branch of fundamental solitons for $D > 0$, and with no solitary waves at all for $D < 0$. Within the gap, we find infinite sequences of two-solitons that are bound states (BS's) of the fundamental ones. Although likely to be dynamically unstable [7], BS's are worth studying to

delimit the existence domain of fundamental solitons; see Figs. 2 and 4 below.

The generalized MTM including dispersion terms is

$$iu_t + iu_x + Du_{xx} + (\sigma|u|^2 + |v|^2)u + v = 0, \quad (1)$$

$$iv_t - iv_x + Dv_{xx} + (|u|^2 + \sigma|v|^2)v + u = 0, \quad (2)$$

where $u(x, t)$ and $v(x, t)$ are the complex amplitudes of the counterpropagating waves, x and t are the coordinate and time, D is the coefficient of spatial dispersion, and σ is the relative SPM coefficient, which is zero for MTM and $\frac{1}{2}$ for the OM case. Besides fibers with grating, the models (1) and (2) can be applied to stationary fields in two parallel tunnel-coupled planar nonlinear waveguides. In that case t and x are the propagation distance and the transverse coordinate, respectively, the terms $\pm iu_x$ account for misalignment of optical axes in the two cores, D is an effective diffraction (not dispersion) coefficient, and the CPM terms must be omitted (see, e.g., [8]). Actually, the latter realization of the model is closer to experiment, as optical axes misalignment is a powerful control parameter enabling rescaling of physically realistic systems into the forms (1) and (2) [8]. In contrast, for fibers with grating, a simple estimate shows that dispersion may not be conspicuous, unless the spatial width of the soliton is comparable to the grating period, i.e., the wavelength of light, when Eqs. (1) and (2) are not applicable [9].

Essentially the same model governs interaction of two circular polarizations of light in a nonlinear fiber, in which the linear coupling is induced by the birefringence, and the group-velocity difference by a fiber's twist (see the review [10]). In untwisted fibers, interaction between linear polarizations is described by similar models, but with linear coupling replaced by a cubic four-wave-mixing term (see [11] for a family of walking solitons in the latter

model). Our approach is different; instead of starting from solitons of decoupled nonlinear Schrödinger equations with the couplings treated as perturbations, we start from the TS of the strongly coupled system with dispersion or diffraction being a perturbation.

Being interested here only in the zero-velocity solitons, we substitute into Eqs. (1) and (2) $u(x, t) = e^{-i\omega t}U(x)$, $v = e^{-i\omega t}V(x)$ to obtain the coupled ordinary differential equations (ODEs)

$$DU'' + iU' + \omega U + (\sigma|U|^2 + |V|^2)U + V = 0, \quad (3)$$

$$DV'' - iV' + \omega V + (|U|^2 + \sigma|V|^2)V + U = 0, \quad (4)$$

the prime standing for d/dx . In this notation, the TS occur at $D = 0$ and $|\omega| < 1$. Equations (3) and (4) are equivalent to an eighth-order dynamical system with two integrals of motion: the Hamiltonian

$$\begin{aligned} H = & D(|U'|^2 + |V'|^2) + \omega(|U|^2 + |V|^2) \\ & + (\sigma/2)(|U|^4 + |V|^4) \\ & + |U|^2|V|^2 + (UV^* + VU^*), \end{aligned} \quad (5)$$

and the ‘‘angular momentum,’’ generated by invariance with respect to the continuous phase transformation,

$$\begin{aligned} M = & D(UU'^* - U^*U' + VV'^* - V^*V') \\ & + |V|^2 - |U|^2. \end{aligned} \quad (6)$$

This Hamiltonian system has several discrete symmetries: the odd symmetry $Z: (U, V) \rightarrow (-U, -V)$, two other \mathbb{Z}_2 ones $Z_1: U \leftrightarrow V^*$, $Z_2: U \leftrightarrow -V^*$, and four reversibilities

$$R: (U, U', V, V') \rightarrow (U^*, -U'^*, V^*, -V'^*), : x \rightarrow -x, \quad (7)$$

$$S: (U, U') \leftrightarrow (V, -V'), : x \rightarrow -x, \quad (8)$$

along with their odd images ZR and ZS .

The first step in locating solitary waves is to solve the linearized problem, assuming solutions $\sim e^{\lambda x}$. This problem, solved *exactly*, gives a set of double eigenvalues:

$$(D^2\lambda^4 + 2D\omega\lambda^2 + \lambda^2 + \omega^2 - 1)^2 = 0. \quad (9)$$

Equation (9) defines four regions on the plane $\{D, \omega\}$ with different types of eigenvalues (see Fig. 1). Solitary waves with exponentially decaying tails are possible only in regions I, II, and III (and their images for $D < 0$), where eigenvalues with nonzero real part occur.

We notice that Eqs. (3) and (4) are compatible with the reduction $U = V^*$. This results in a single equation for $U(x)$,

$$DU'' + iU' + \omega U + (1 + \sigma)|U|^2U + U^* = 0, \quad (10)$$

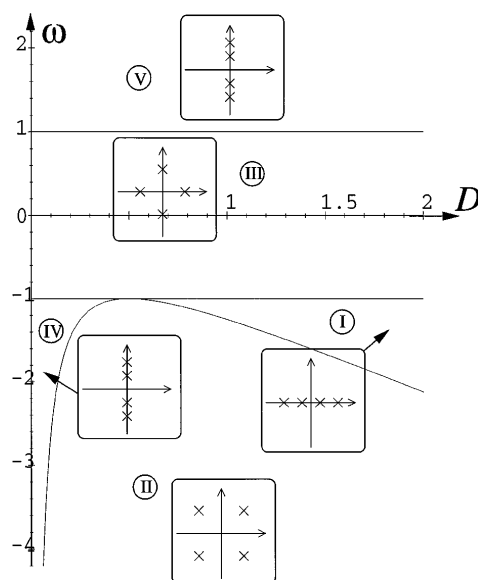


FIG. 1. Parameter regions for $D > 0$ with different types of eigenvalues of the linearized Eqs. (3) and (4), as illustrated by the insets. The curve delimiting region II is $D + 1/4D - \omega = 0$. At the point $D = 1/2$, the curve is tangent to the horizontal $\omega = -1$. The picture for $D < 0$ is obtained by rotating the figure by 180° .

equivalent to a real four-dimensional ODE system. All the zero-velocity solitons in MTM and OM obey exactly the same reduction, and a simple argument based on consideration of the unstable manifolds shows that *all* possible zero-velocity solitons to (1) and (2) within region II are trivially related to solutions of (10) by rotation in the (U, V) plane. Henceforth, we set $\sigma = 0$, because σ can be scaled out from Eq. (10). Furthermore, for Eq. (10), $S \equiv R$, and the angular momentum (6) identically vanishes. The eigenvalues of the corresponding linearized equation are given by Eq. (9), but are all single; i.e., Fig. 1 remains fully relevant.

The soliton is a homoclinic-to-zero solution to Eq. (10). According to general theorems [12], in region III, where $U = 0$ is a saddle-center fixed point, homoclinic trajectories that are symmetric under a reversibility are of codimension one (nonsymmetric homoclinic trajectories are of codimension two). Hence, solutions can exist only on isolated curves in the $\{D, \omega\}$ parameter plane, the number of which may be finite or infinite. Moreover, given a sign condition on the quadratic part of the Hamiltonian, each curve will be accompanied by an infinite accumulation of curves on which BS's exist [12]. In contrast, in regions I and II, where the fixed point $U = 0$ is hyperbolic, homoclinic trajectories are generic, i.e., they occur uniformly in two-dimensional parameter regions [13]. But region III is of most interest, as it abuts the segment $\{D = 0, |\omega| < 1\}$ on which the TS solitons exist.

To obtain solutions, we use robust numerical methods for solving two-point boundary-value problems on a truncation of an infinite x interval with boundary conditions placing the solution in the stable or unstable eigenspaces

at the origin; see [14], and references therein. Continuation of solutions, with respect to parameters, is carried out using the software AUTO [15], specifically exploiting the reversible structure of (10).

Our main findings are summarized in Fig. 2. Here, three solid curves represent the isolated loci of fundamental or *primary* (single humped, in one component) solitons, and the dashed curves are a small sample of loci of their two-humped BS's. All primary solitons are reversible with respect to the transformation ZR , see Eq. (7); we have found no evidence of any R -reversible solutions. In panel (b), we use, instead of the frequency ω , the soliton's energy $E = \int_{-\infty}^{+\infty} |U(x)|^2 dx$. Typical examples of one solitons are displayed in Fig. 3, and typical two-humped BS's are shown in Fig. 4 (only half of each two-soliton is shown in this figure).

Each of the primary branches in Fig. 2 (labeled 1–3) appears to bifurcate at zero soliton amplitude from the line $\omega = 1$, although there are numerical difficulties in computing right up to this singular limit. The D values of these three bifurcations at $\omega = 1$ are $D = 0.50, 0.20$, and 0.11 to two decimal places. A straightforward calculation of the sign condition in [12] on the Hamiltonian (5) implies that curves of ZR -reversible BS's must accumulate on each of the primary curves from both sides (e.g., we have found

BS branches 9–12 and 4 and 5 accumulating on branch 1 from the right and left, respectively). Branches 9–12 are also part of a larger sequence we have computed which for fixed D accumulates on $\omega = 1$.

Three-solitons and higher-order BS of the primary solitons can also be found, the three-humped ones accumulating on two-solitons, etc. in accord with the theory [12]. We do not describe these objects, because it is unlikely that even the two-solitons may be dynamically stable in systems (1) and (2), while stability of the primary solitons is quite feasible [7]. However, stability analysis is deferred to another work. Homoclinic solutions were also sought for $D < 0$ and $|\omega| < 1$, but no evidence of primary or multihumped ones was found.

Looking at Fig. 2, there remains the crucial question whether there are any more primary branches to the left of that labeled 3. A seemingly plausible conjecture is that there is a self-similar structure of primary branches as one moves to the left in Fig. 2, i.e., infinitely many branches accumulating on the TS segment $\{D = 0, |\omega| < 1\}$, the branches 1, 2, and 3 being but the first three in the structure (note that, at least for $D < 2$, there cannot be any further primary solutions to the *right* of branch 1, because here the two-soliton curves 9–12 form a barrier for them). However, careful numerical scanning of the parametric plane of Fig. 2 to the left of branch 3 has strongly indicated that the above hypothesis is *false*, in region III there being *no* primary branches other than 1, 2, and 3. For ω sufficiently close to -1 , this assertion is substantiated as follows.

Figure 4 reports the results of a thorough numerical investigation of other possible solution branches at $\omega = -0.99$, varying D between 0 and $\frac{1}{2}$. We find that, to the left of branch 3, an infinite sequence of *multisoliton* BS's occurs. Even though, because of numerical problems in the singular limit, we have computed only the corresponding two-solitons down to $D \approx 0.2$, Fig. 4 clearly suggests accumulation of the sequence as $D \rightarrow 0$. The energy of the two-solitons remains finite, while the separation between the two bound pulses diverges $\sim 1/D$ as $D \rightarrow 0$ (which explains the existence of TS in the limit $D = 0$). Thus, what does accumulate on the TS manifold at $D \rightarrow 0$ is an infinite sequence of multisoliton branches, with no

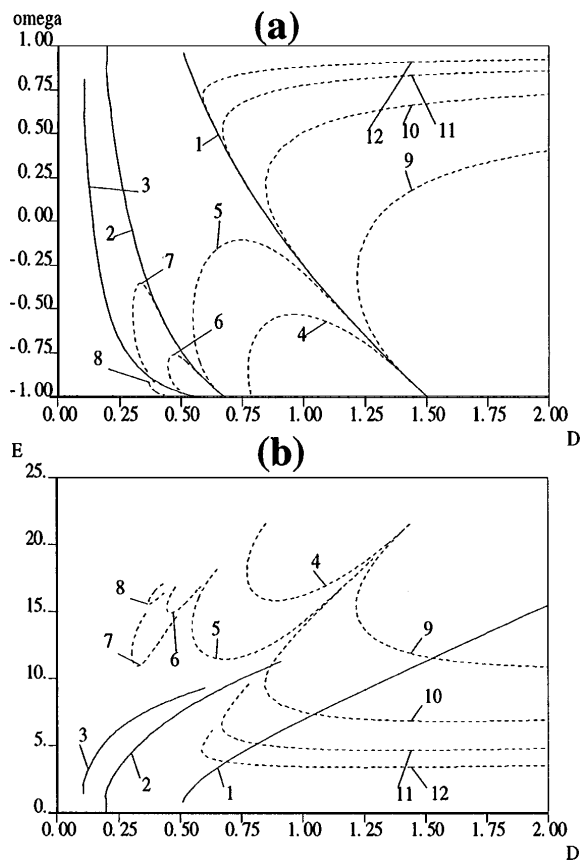


FIG. 2. A two-parameter bifurcation diagram for fundamental solitons (solid curves) and two-soliton bound states (dashed curves) on the planes (D, ω) (a), and (D, energy) (b).

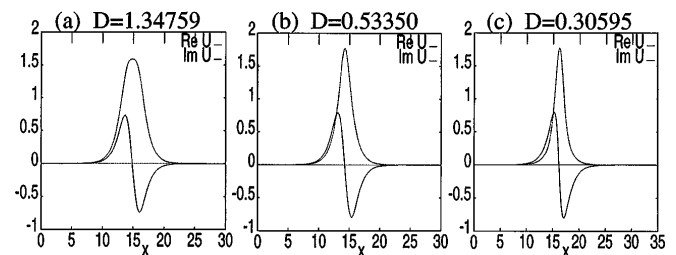


FIG. 3. The fundamental solitons at the points of intersection of the primary-soliton branches (Fig. 2) by the line $\omega = -0.8$. (a), (b), and (c) correspond to 1, 2, and 3 branches, respectively, in Fig. 2.

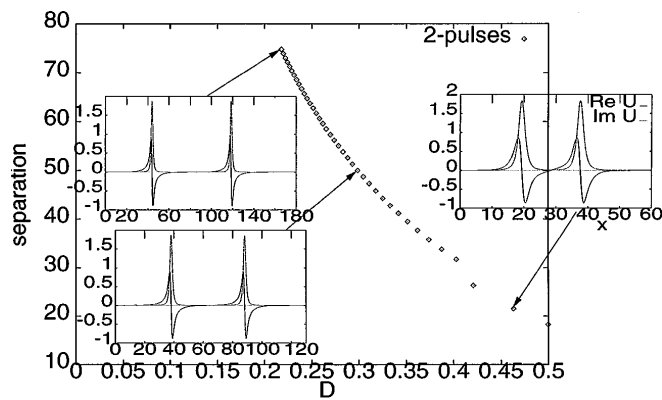


FIG. 4. A sequence of two-soliton solutions at $D \rightarrow 0$ for $\omega = -0.99$. The insets show the shape of the solutions.

fundamental-soliton branch closer to the TS manifold than the branch 3 in Fig. 2.

To support this numerical finding with qualitative arguments, consider what happens to the primary branches as they cross the line $\omega = -1$ from above. For $D > \frac{1}{2}$ this is a “harmless” transition, because the real eigenvalues of the linearized equations that govern the decay of the homoclinic solution at $|x| \rightarrow \infty$ behave smoothly, and they are bounded away from zero. A well-defined primary branch safely crosses $\omega = -1$ in this case, which for $\omega < -1$ describes a curve of “orbit-flip” bifurcations (cf. [16]). However, for $D < \frac{1}{2}$, the corresponding eigenvalues vanish as $\omega \rightarrow -1$, hence, no smooth transition can take place. Thus, there may be *no* primary-soliton branches at $0 < 1 + \omega \ll 1, D < \frac{1}{2}$.

The most important result of this work is that there is a *finite gap* separating TS, existing in the singular limit $D = 0$, from new solitons at $D \neq 0$. Thus, the Thirring solitons are *structurally unstable* against adding the dispersion or diffraction. A natural question is if there is a gap for solitons at a finite velocity. Preliminary numerical results give a positive answer, which is further supported by an argument that solutions to the ODEs describing the soliton’s shape continuously depend on the parameters (including velocity), except at a singular point. The addition of dispersion to MTM is, obviously, a singular perturbation because it doubles the system’s order; however, nonzero velocity is not a singular perturbation.

We mention finally results for solitons in regions I and II. As stated, here homoclinic solutions are generic, and a primary-soliton branch can be path followed continuously for all ω and D inside regions I and II. Inside region II it develops oscillations in its tails due to the complex eigenvalues. At the boundaries between regions I and III and II and IV, the solution disappears through a zero-amplitude bifurcation, as predicted by the appropriate normal-form analysis [17]. Other primary-soliton solutions have more complicated bifurcation diagrams; in both regions I and II, two- and multisoliton BS’s also occur. A detailed description of the complete bifurcation structure will be given elsewhere.

Since the original submission of this paper, we have become aware of the preprint [18] containing new results on the *dynamical* stability of the solitons in OM *without* the dispersion terms. They demonstrate that, except for the integrable Thirring model case, all the solitons are subject to an instability which is too weak to have been observed in earlier numerical simulations. Note that a similar instability mechanism for solitons of OM was predicted nonrigorously in [19] using a variational approximation. A dynamical stability analysis for the new solitons in the presence of dispersion found in the present work will be presented elsewhere.

We appreciate valuable discussions with Y. S. Kivshar, G. G. Luther, and D. E. Pelinovsky.

- [1] W. E. Thirring, Ann. Phys. (N.Y.) **3**, 91 (1958).
- [2] A. V. Mikhailov, Pis'ma Zh. Eksp. Teor. Fiz. **23**, 356 (1976) [JETP Lett. **23**, 320 (1976)]; D. J. Kaup and A. C. Newell, Lett. Nuovo Cimento **20**, 325 (1977).
- [3] D. N. Christodoulides and R. I. Joseph, Phys. Rev. Lett. **62**, 1746 (1989).
- [4] A. Aceves and S. Wabnitz, Phys. Lett. A **141**, 37 (1989).
- [5] B. J. Eggleton, R. E. Slusher, C. Martijn de Sterke, P. A. Krug, and J. E. Sipe, Phys. Rev. Lett. **76**, 1627 (1996).
- [6] L. Torner, D. Mazilu, and D. Mihalache, Phys. Rev. Lett. **77**, 2455 (1996).
- [7] Y. Silberberg and Y. Barad, Opt. Lett. **20**, 246 (1995).
- [8] W. Mak, B. A. Malomed, and P. L. Chu, Phys. Rev. E **55**, 6134 (1997).
- [9] E. Granot, S. Stenklar, B. Malomed, Y. Isbi, and A. Lewis, Opt. Lett. **22**, 1290 (1997).
- [10] M. Romagnoli, S. Trillo, and S. Wabnitz, Opt. Quantum Electron. **24**, S1237 (1992).
- [11] J. M. Soto-Crespo, N. Akhmediev, and A. Ankiewicz, Phys. Rev. E **51**, 3547 (1995); L. Torner, D. Mihalache, D. Mazilu, and N. Akhmediev, Opt. Commun. **138**, 105 (1997).
- [12] A. Mielke, P. Holmes, and O. O'Reilly, J. Dyn. Differ. Equ. **4**, 95 (1992).
- [13] R. L. Devaney, J. Differ. Equ. **21**, 431 (1976); B. Buffoni, A. R. Champneys, and J. F. Toland, J. Dyn. Differ. Equ. **8**, 221 (1996).
- [14] E. J. Doedel, M. J. Friedman, and B. I. Kunin, Numer. Algorithms **14**, 103 (1997); A. R. Champneys, Yu. A. Kuznetsov, and B. Sandstede, Int. J. Bifurcation Chaos **6**, 867 (1996), and references therein.
- [15] E. J. Doedel, A. R. Champneys, T. R. Fairgrieve, Yu. A. Kuznetsov, B. Sandstede, and W. Wang, AUTO97 Continuation and Bifurcation Software for Ordinary Differential Equations, 1997. Available by anonymous ftp from ftp.cs.concordia.ca, directory pub/doedel/auto.
- [16] B. Sandstede, C. K. R. T. Jones, and J. C. Alexander, Physica (Amsterdam) **106D**, 167 (1997); A. R. Champneys and M. D. Groves, J. Fluid Mech. **342**, 199–229 (1997).
- [17] G. Iooss, Fields Inst. Comms. **4**, 201 (1995).
- [18] I. V. Barashenkov, D. E. Pelinovsky, and E. V. Zemlyanaya (to be published); JINR Report No. E17-98-7 (Dubna, Russia).
- [19] B. A. Malomed and R. S. Tasgal, Phys. Rev. E **49**, 5787 (1994).